Sensors & Actuators: B. Chemical 393 (2023) 134227

Contents lists available at ScienceDirect

Sensors and Actuators: B. Chemical

journal homepage: www.elsevier.com/locate/snb

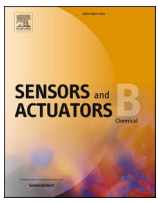

Direct recording of action potentials of cardiomyocytes through solution processed planar electrolyte-gated field-effect transistors

Adrica Kyndiah [a,*,1], Michele Dipalo [b,1], Alireza Molazemhosseini [a], Fabrizio Antonio Viola [a,2], Francesco Modena [a], Giuseppina Iachetta [b], Nicolas F. Zorn [c], Felix J. Berger [c], Jana Zaumseil [c], Mario Caironi [a,*], Francesco De Angelis [b,*]

[a] Center for Nano Science and Technology, Istituto Italiano di Tecnologia, Via Rubattino 81, 20134 Milano, Italy
[b] Istituto Italiano di Tecnologia, Via Morego 30, 16163 Genova, Italy
[c] Institute for Physical Chemistry, Ruprecht-Karls Universität Heidelberg, Im Neuenheimer Feld 253, 69120 Heidelberg, Germany

ARTICLE INFO

Keywords:
Bioelectronics
Electrolyte-gated transistors
Cardiac cells
Intracellular potential
Semiconducting carbon nanotubes

ABSTRACT

To achieve intracellular recording of action potentials by using simple devices that can be easily fabricated and processed is crucial in cardiology and neuroscience. Present tools and technology include invasive patch clamp technique, 3D nanostructures often combined with electro/opto poration methods and nanodevices such as nanowire field-effect transistors. However, these approaches mostly require complex manufacturing processes or are invasive. In this work, we report the spontaneous intracellular-like recording of cardiac cells using a cost-effective, planar Electrolyte-Gated Field-Effect Transistor (EGFET) based on solution-processed polymer-wrapped monochiral semiconducting single-walled carbon nanotubes (SWCNTs). By simply turning on the transistor, spontaneous recordings of intracellular-like action potentials of human induced pluripotent stem cells derived cardiomyocytes are enabled. In addition, we demonstrate that the same planar EGFET can also be employed as a platform for electroporation with significant device performance and cell viability. The simplicity of the device combined with the high signal to noise ratio opens up new opportunities for low-cost, reliable, and flexible biosensors and arrays for high quality parallel recording of cellular action potentials.

1. Introduction

Bioelectronic recording platforms aimed at measuring the electrophysiological activity (action potentials) of excitable cells, such as neurons and cardiomyocytes, are continuously developing in the field of electrophysiology. The amplitude, shape and duration of Action Potentials (APs) provide relevant information on the state of the ion channels that are present on the cell membrane [1], which then indicates the physiological condition and health of the cell. Techniques to measure electrophysiological activity of cells or tissues in a non-invasive way varies from electrodes, such as the commercially available Microelectrode Arrays (MEA) [2], to Field-Effect Transistor (FETs) [3,4]. Compared to MEAs, FETs offer an intrinsic amplification of the signal thus improving the signal to noise ratio [5]. Besides, FETs can be easily downscaled for improved spatial resolution as compared to MEAs whose impedance increases with a decreasing area. The advantage in using non-invasive methods is related to the vitality of the cells that is not compromised during the electrical recording, thus allowing multiple and long duration recordings that are fundamental for chronic studies [6]. To enable recordings of APs from large ensembles of cells on MEAs and FETs, various methods have been recently developed, which include the use of structured 3D micro or nano devices [7–13] that can mechanically perforate or form a tight seal onto the cell membrane. Electroporation [14,15] and plasmonic optoporation methods [16,17], which use electrical or optical pulses to perforate the cell membrane in a relatively non-invasive manner, have also demonstrated to be successful in acquiring intracellular action potentials without any mechanical penetration. Beside performance considerations, another relevant aspect that has to be considered is the fabrication simplicity and ease of deployment of the active electronic interfaces. In most cases, the

* Corresponding authors.
E-mail addresses: adrica.kyndiah@iit.it (A. Kyndiah), mario.caironi@iit.it (M. Caironi), Francesco.DeAngelis@iit.it (F. De Angelis).
[1] These authors contributed equally.
[2] Present address: Department of Electrical and Electronic Engineering - University of Cagliari, Via Marengo 3, 09123 Cagliari, Italy.

https://doi.org/10.1016/j.snb.2023.134227
Received 21 March 2023; Received in revised form 8 June 2023; Accepted 27 June 2023
Available online 28 June 2023

fabrication of 3D nanostructures or nanowire FETs require a complex fabrication process that hardly satisfies cost and production requirements of biosensors or medical devices. In addition, the material properties of the electronic transducers to be interfaced with biological cells should meet the necessary requirements such as mechanical flexibility, biocompatibility and long term stability in aqueous electrophysiological environment. To this end, organic and carbon-based materials become excellent candidates for bioelectronic transducers [18].

Recently, Electrolyte-Gated Field-Effect Transistors (EGFETs) based on organic and carbon-based materials have shown great potential for application in cell recording and stimulation [5,19–22]. The biocompatibility and mechanical properties of such materials favour their interaction with biological systems [18,23]. Their flexibility and conformability make them ideal for in-vivo applications, prosthetics, and wearable devices [24]. Most importantly, since these materials can be easily processed using solution and printing techniques, the cost and effort required for the fabrication of the devices is greatly reduced as compared to conventional Complementary Metal-Oxide Semiconductor (CMOS) technology, both in terms of capital expenditures and in terms of energy consumption [25]. This makes them an excellent candidate in the pharmaceutical industry for their application in drug testing [26,27], besides offering new opportunities for investigation tools in research activities, i.e. cost-effective and customized large-area arrays for cell cultures monitoring.

The working principle of EGFETs rely on the capacitive coupling of the gate/electrolyte and electrolyte/semiconductor interface [20,21,28,29]. The high sensitivity of the devices to small potential variations at the semiconductor/electrolyte interface makes them in principle ideal for recording the electrical activity of electrogenic cells. EGFETs are planar devices whose active channel is in direct contact with the cells. The change in the transmembrane potential of the cell is transduced in the effective change of the applied gate voltage, which is reflected on the modulation of the source-drain current [19]. The high electrical performance of these transistors together with their biocompatibility and device stability in aqueous environment make them a strong candidate for bioelectronics recording platform [30]. To this end, a class of EGFETs called Organic Electrochemical Transistors (OECTs), which consist of ion permeable semiconductors, have been employed for electrophysiological recordings. Compared to EGFETs, OECTs have a higher transconductance due to the volumetric field-effect, but have a relatively slower time response due to the penetration of ions to modulate the conductivity of the semiconductor. So far, OECTs can record extracellular-like potential signals, similar to those obtained with MEAs, while intracellular-like signals can be recorded with OECTs only when electroporation is performed [31]. In the absence of an external stimuli, EGFETs have only been able to record the extracellular field potentials of the cells, indicating a limit in the coupling. In fact, direct measurement of action potentials, i.e. as obtained in intracellular recordings, has not been achieved thus limiting the applications of EGFETs in electrophysiology.

In this work, we demonstrate that an EGFET based on solution processed polymer sorted wrapped monochiral semiconducting Single-Walled Carbon Nanotubes (SWCNTs), can be employed for the spontaneous in vitro recordings of action potentials of human induced pluripotent stem cells derived cardiomyocytes (hiPSC-CMs). The active channel of the device consists of a random network of SWCNTs, which can be simply obtained by spin coating or printing, without requiring complex manufacturing. We recently reported that planar EGFETs based on solution-processed SWCNTs are highly stable in water media, thus offering a reliable platform for biosensing [32], and monitoring of cell proliferation and detachment processes in electrophysiological conditions [33]. Here, hiPSC-CMs were cultured directly on the EGFETs and bioelectrical recordings of intracellular-like cardiac APs were obtained by simply turning on the transistors at their maximum transconductance. Spontaneous recording of intra-cellular like APs could not be consistently achieved before with simple planar transistors channels configurations. Remarkably, the amplitude and shape of the recorded intracellular-like potential is at par with the state-of-the-art techniques that would require complex fabrication and external stimuli. In addition, we show that, in combination to spontaneous recording, EGFETs can also be employed to electroporate the cells on demand and multiple times without affecting cell viability. This way, EGFETs can repeatedly record the electrical activities at intracellular level with high accuracy, thus paving the way for their exploitation in electrophysiological studies.

2. Experimental section/Methods

2.1. Preparation of (6,5) SWCNT dispersions

(6,5) SWCNT dispersions were prepared from CoMoCAT® carbon nanotubes (Chasm Advanced Materials, SG65i-L58). According to the supplier, this CoMoCAT material has a maximum carbon content of 95%, and 93% of which are SWCNTs. 40% of the nanotubes are (6,5) SWCNTs, therefore ~35 wt% of the raw material. Shear force mixing (SFM) was used for selectively dispersing (6,5) SWCNTs through polymer-wrapping using poly[(9,9-dioctylfluorenyl-2,7-diyl)-*alt*-*co*-(6,6′-(2,2′-bipyridine))] (PFO-BPy) [34]. Briefly, 0.5 g/L PFO-BPy (American Dye Source, M_W = 40 kg/mol) were dissolved in toluene before adding 0.4 g/L CoMoCAT raw material. SFM using a Silverson L2/Air mixer was then applied at maximum speed (10,230 rpm) for 72 h at a temperature of 20 °C. Next, the dispersion was centrifuged twice for 45 min at 60,000 *g* and the supernatant was collected and passed through a poly(tetrafluoroethylene) (PTFE) syringe filter (pore size 5 μm) to remove undispersed material and aggregates. To collect the SWCNTs, the resulting dispersion was filtered through a PTFE membrane (Merck Millipore, JVWP, 0.1 μm pore size) and washed with toluene in order to remove excess polymer. The nanotubes ink was prepared through redispersion of the SWCNT filter cake in toluene by 30 min of bath sonication, obtaining an optical density of 10 cm^{-1} at the E_{11} transition.

2.2. Device fabrication

An array of transistors consisting of interdigitated source-drain electrodes with channel length of 3 μm and channel width of 146 μm and 64 μm were patterned on a glass substrate by mask-less reverse lithography process (AZ5214 photoresist using MLA100 Heidelberg mask-less aligner) followed by thermal evaporation of chromium (2 nm)/ gold (15 nm) and lift-off in N-methyl-2-pyrrolidone. Gold electrodes were subjected to 3 min of oxygen plasma treatment at 100 W and semiconducting SWCNTs dispersion made in toluene (concentration of (6,5) SWCNTs of 18 mg L^{-1}, corresponding to an optical density of 10 cm^{-1} at the E_{11} absorption peak) was spincoated on the chip. Three passes of spincoating were done in nitrogen glovebox and each pass was followed by 1 min annealing at 100°C. Spincoated semiconductor layer was then rinsed with tetrahydrofuran, isopropanol and dried with a nitrogen flux. A film of inkjet-printed biocompatible insulator (SU8 – TF6001 MicroChem) was employed to selectively passivate source and drain electrodes.

2.3. Characterization of EGFETs and cell recording

The electrical performance of the SWCNT EGFETs was measured using cell medium (iCell Cardiomyocytes Maintenance Medium) as an electrolyte and platinum wire as the gate electrode for applying the gate bias. To check the electrical performance of the transistor, a transfer curve is acquired using Agilent 2912B source meter. Gate voltage V_{GS} is swept from + 0.2 V to − 0.8 V, keeping the V_{DS} constant at − 0.5 V. To measure the response time of the transistor, we applied a fast square pulse to the gate bias (from −0.7 to −0.6 V) for a duration of 1 ms. The time response τ is obtained by fitting an exponential $I_{DS} \approx e^{-t/\tau}$ to the

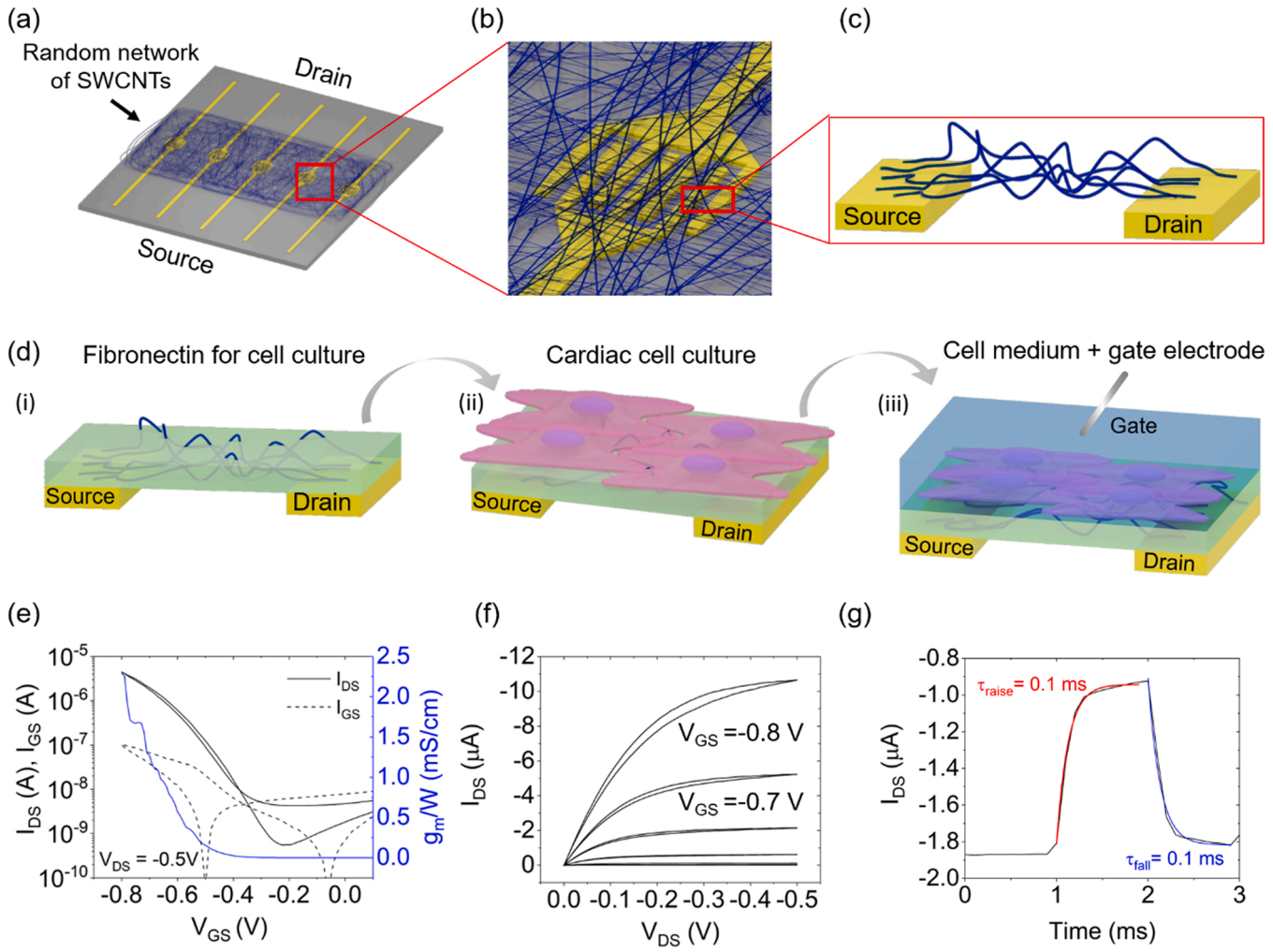

Fig. 1. EGFETs architecture and their electrical characteristics in the presence of cardiac cells. (a). Sketch of the EGFET array with several FETs in a linear array. (b) Close-up sketch of interdigitated contacts with SWCNTs on top. (c) Sketch of SWCNTs network bridging across source and drain contacts. (d) (i) Coating of the FET with fibronectin prior to cell culture. (ii) Cardiac cells plated on the FETs. (iii) Sketch of the final configuration of EGFETs with cardiac cells where the cell medium acts as an electrolyte and a platinum wire immersed act as a gate electrode. (e) Source-Drain Current I_{DS} and leakage current I_{GS} versus Gate-Source Voltage V_{GS} transfer characteristic curves of the EGFETs in electrophysiological condition and in the presence of living cardiac cells. (f) Corresponding output characteristic curves. (g) Response time ($\tau = \tau_{raise} + \tau_{fall} = 0.2$ ms) of the transistor current I_{DS} to a gate voltage variation of 0.1 V with $V_{DS} = -0.5$ V.

output of the I_{DS}.

For bioelectronics recording, V_{GS} is then fixed at a bias point where the EGFET has maximum transconductance g_m. Keeping the V_{DS} constant at − 0.5 V, I_{DS} is recorded over time. The data obtained is then post processed by using the asymmetric baseline smoothing to eliminate the drift in the current. No other filter is applied in the raw data acquired. After each recording, an I-V transfer curve is taken in order to check the stability of the device. The recordings reported in this work are obtained from 6 different transistors, in 3 different cell culture preparations, in 3 different measurement sessions.

2.4. Cell culture on the EGFETs

Human induced pluripotent stem cell-derived cardiomyocytes (hiPSC-CMs) were purchased from Cellular Dynamics International (CDI). hiPSC-CMs were plated directly on EGFETs (30,000 cells for device) coated with fibronectin (Corning) for 1 h at 37 °C, 5% CO_2 in a humidified incubator. EGFETs were previously sterilized in 70% ethanol for 30 min followed by three washes with sterile water. The cells were cultured on the devices and electrophysiological recordings were performed 10–14 days after plating according to the specifications of CDI.

2.5. Live/Dead assay

Cell viability after electroporation and intracellular recording was tested using Live/Dead assay kit (Thermo Fisher Scientific, L3224). Briefly, live cells are stained with calcein acetoxymethyl (green fluorescence), whereas dead cells with ethidium homodimer (red fluorescence). The cells were imaged with a Nikon Eclipse FN1 microscope by using a 20x air objective and filters for FITC channel and TRITC channel.

2.6. Immunofluorescence with Troponin T

To demonstrate the biocompatibility of the -SWCNT layer, immunofluorescence for cardiac troponin-T (TNNT2/cTnT) was performed on hiPSC-CMs after 14 days in vitro (DIVs) as described in Dipalo et al., 2021 [35]. Briefly, the cells were fixed with 4% (w/v) formaldehyde in DPBS for 15 min, incubated with the permeabilization solution (1% Saponin in DPBS) for 15 min and then incubated with a blocking solution (3% bovine serum albumin) for 30 min. Thereafter, hiPSC-CMs were incubated with a primary antibody (mouse anti-TNNT2 A25969) diluted 1:1000 in the blocking solution for 3 h followed by washing 3 times with wash buffer and incubation with secondary antibody (Alexa

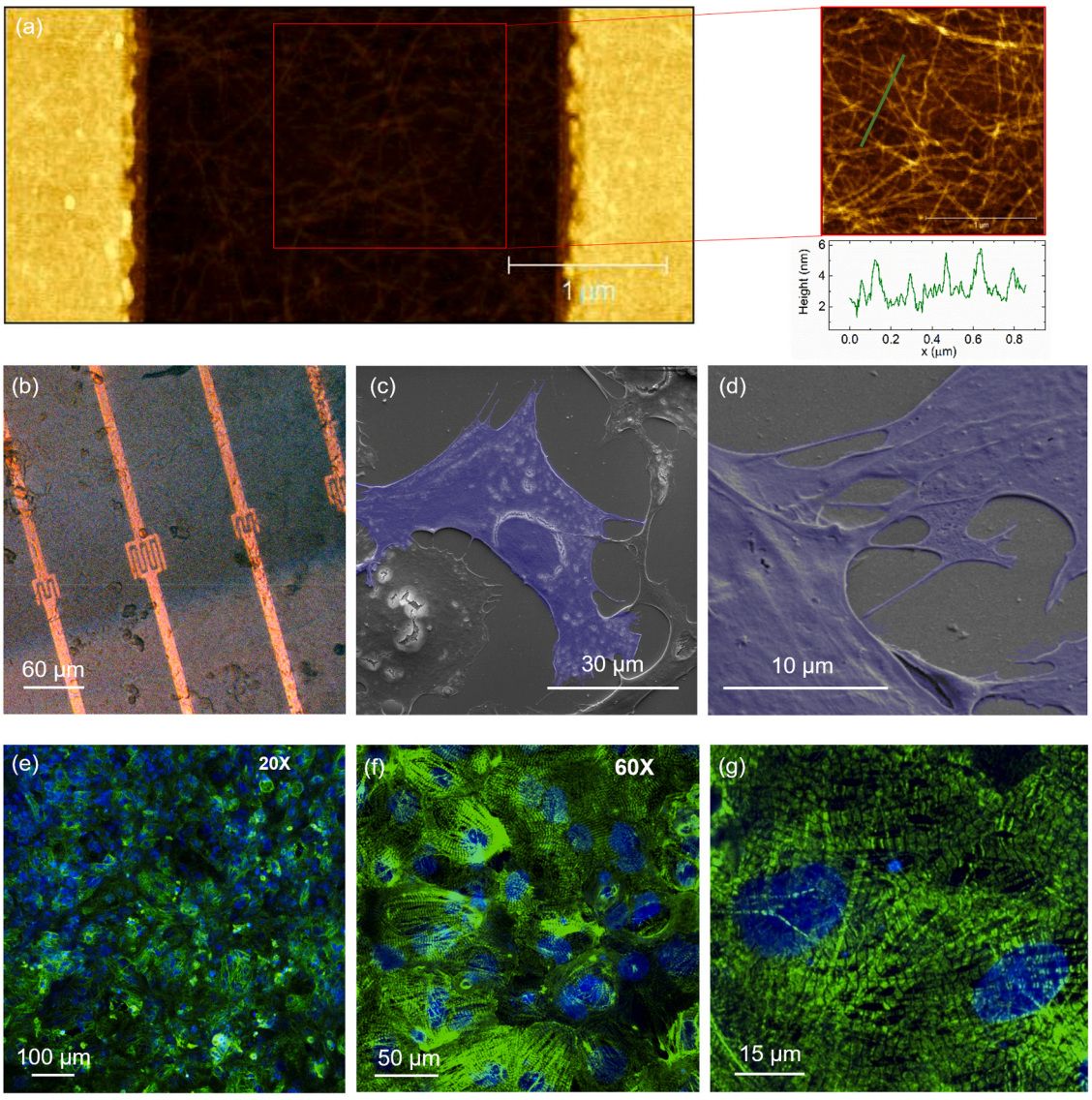

Fig. 2. Cardiac cell characterization on EGFETs (a) AFM map of an EGFET with magnified view of the channel in the inset on right side. (b) Bright-field image of interdigitated EGFETs with cultured live hiPSC-CMs on top. (c) SEM image of hiPSC-CMs cultured and fixated on SWCNT layer. (d) SEM detail of spindle like connections between two cardiomyocytes on SWCNT layer. (e-g) Immunofluorescence images at different magnifications of hiPSC-CMs on SWCNT layer.

Fluor 488 donkey anti-mouse) diluted 1:250 in blocking solution for 1 h. Finally, cell nuclei were counterstained with DAPI and images were acquired using an inverted Nikon Confocal A1 microscope.

2.7. Scanning electron microscopy (SEM)

hiPSC-CMs on SWCNTs were fixed with a solution of 2% glutaraldehyde in Na cacodylate buffer (0.1 M) for 2 h, washed for three times with the same buffer, post-fixed in 0.1% osmium tetroxide for 1 h and then rinsed twice with deionized water. Subsequently, the samples were dehydrated with a graded series of alcohol, followed by incubation in ethanol:hexamethyldisilazane (HMDS) and then in 100% HMDS. Finally, the samples were dried overnight in air and coated with a 10 nm gold layer. Imaging analysis was performed using a dual beam Helios Nanolab600 by ThermoFisher.

3. Results and discussion

3.1. EGFETs with cardiac cells and their electrical characteristics in electrophysiological environment

The device architecture of our EGFETs is depicted in Fig. 1a, b and c. The active channel of the transistor consists of a spin coated random network of solution-dispersed SWCNTs that bridges the source and drain gold electrodes (Fig. 1(c)). Fibronectin gel is drop casted onto the channel of the transistor prior to cell culture in order to ensure proper adhesion of the cells (Fig. 1(d), panel (i)). Human-induced pluripotent stem cells derived cardiomyocyte (hiPSC-CM) cells are cultured directly on the EGFETs (Fig. 1(d), panel (ii)). The cell medium acts as an electrolyte and the platinum wire immersed in it acts as a gate electrode (Fig. 1(d), panel (iii)). A potential V_{GS} applied between the gate electrode (Pt wire) and the source drives the ions in the electrolyte (cell medium in our case) leading to the formation of an electrical double layer at the distributed SWCNT/electrolyte interface that induces accumulation of holes in the semiconducting layer. A potential V_{DS}

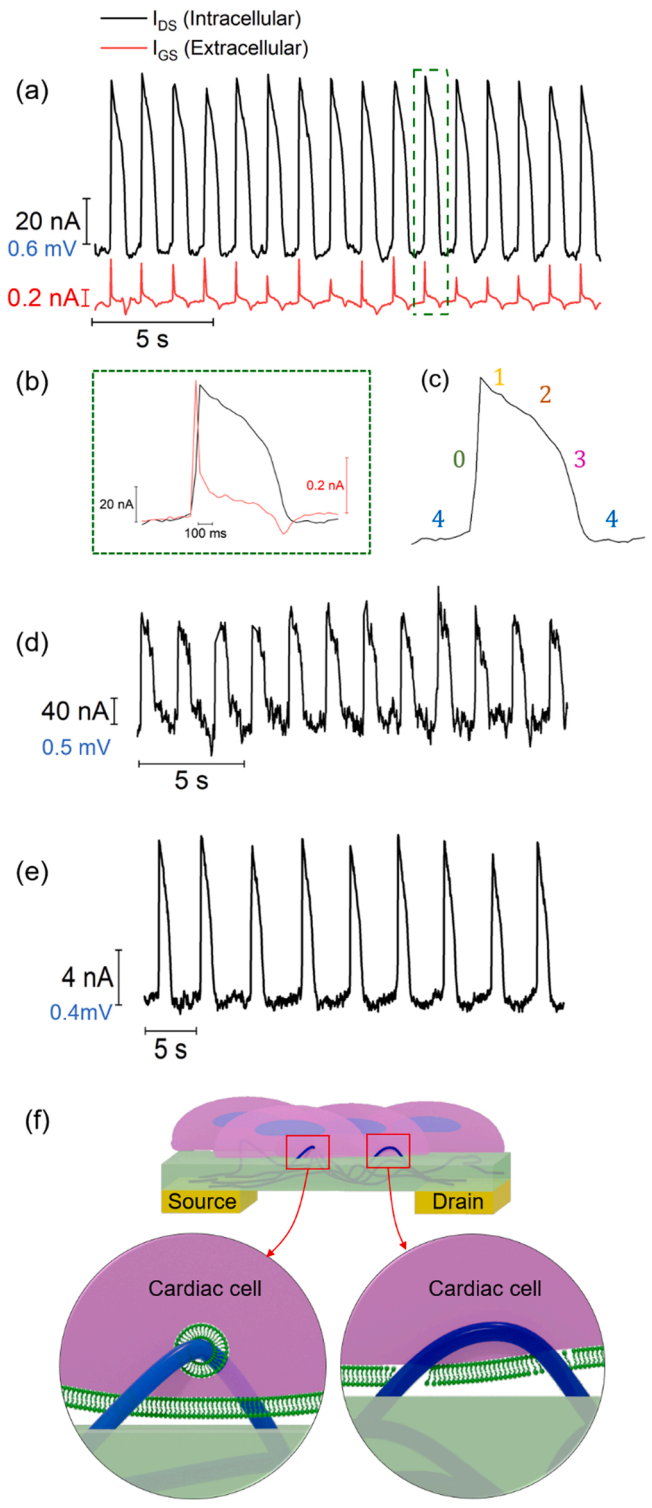

Fig. 3. Bioelectrical recording (a) Black curve represents spontaneous intracellular-like recording of the action potential of hiPSCs cardiomyocytes acquired on the source-drain current traces of EGFETs as a function of time. Red curve is the corresponding spike in the gate current. (b) Zoomed image of the action potential recorded. (c) Cardiac action potential and its corresponding phases of ion channel openings. (d-e) Further exemplary traces of spontaneous intracellular-like recordings of the action potentials of hiPSCs cardiomyocytes acquired on the source-drain current traces of EGFETs (f) Main proposed mechanisms enabling recording of Action Potentials on EGFETs based on SWCNTs.

applied between the source and drain drives these holes across the channel giving rise to the source drain current I_{DS}. The typical transfer characteristic curves of our EGFETs in electrophysiological environment with cells is shown in Fig. 1(e). The normalized transconductance with respect to channel width (g_m/W) of the transistor, as a function of the applied gate bias V_{GS}, is shown in right y-axis (in blue) of Fig. 1(e). An output curve is recorded by sweeping the source-drain voltage V_{DS} at various V_{GS} as illustrated in Fig. 1(f). Our EGFETs work in accumulation mode as evident from the transfer and output characteristic curves. The response time of the EGFETs covered by cells is investigated in Fig. 1(g) by applying a square pulse to the gate bias ($V_{GS} = -0.8$ V; amplitude of pulse: 0.1 V), while keeping the V_{DS} constant. By fitting the rise and fall fronts of the current pulse with an exponential, the time constants $\tau_{raise} = 0.1$ ms and $\tau_{fall} = 0.1$ ms are obtained, respectively. A response time of 0.2 ms makes our EGFETs perfectly suitable for acquiring and transducing biological signals like the action potential.

3.2. Characterization of cardiac cells on EGFETs

The topography of the SWCNT layer can be seen in the atomic force microscopy (AFM) image of Fig. 2(a), where a zoomed image on the channel of the transistor is shown alongside. As it is evident from the images, the spin coated semiconducting channel consists of a random interconnected network of SWCNTs that form continuous charge transport paths from the source to the drain. AFM imaging also indicates that, despite the planar morphology at the microscale, horizontal nanotubes protrude from the surface at the nanoscale and form a matrix that could promote strong cell adhesion. Directly onto the SWCNTs network, an extracellular matrix (fibronectin) is coated prior to plating of hiPSC-CMs on the devices. We show the device consisting of an array of multiple transistors with cells cultured on top in Fig. 2(b). To investigate the growth of hiPSC-CMs on SWCNTs, we also fixated and dehydrated the cardiac cells for imaging with Scanning Electron Microscopy (SEM). The "elongated" and stretched shape of the hiPSC-CMs as observed in the SEM image in Fig. 2(c) evidence good adhesion and health of the cardiac cells onto the SWCNT network. In addition, the SEM image in Fig. 2(d) offers a magnified view of spindle like connections typical of cardiomyocytes. For improved SEM imaging, we used a lower than usual cell density for obtaining isolated cells instead of a closed monolayer.

We further demonstrated the biocompatibility of the SWCNTs layer by immunofluorescence characterization of hiPSC-CMs cultured on the material for 11 *days* in vitro (DIVs). Fig. 2(e, f, g) depicts fluorescence images at 20X and 60X magnifications, which show the filament-like structure of Troponin T, which is typical of matured cardiomyocytes (magnified view in Fig. 2g). The images also depict cell nuclei stained with DAPI.

3.3. Spontaneous recording of the action potential

Approximatively 3 days after culturing cells on EGFETs, the hiPSC-CMs start to spontaneously beat and contract, confirming electrophysiological activity. To record APs, the transistor was turned on at its maximum transconductance, by fixing V_{GS} at (-0.7 ± 0.1) V and V_{DS} at -0.5 V, and I_{DS} was recorded over time. The recorded source drain current I_{DS} at fixed V_{GS} exhibit regular peaks with specific characteristics, as shown in Fig. 3(a). The periodicity of the peaks correspond to the frequency of the beating cells as observed optically (see video in supporting information S1). The change in the transistor current reflects the fact that the transistor is transducing the bioelectrical signal of the cell into an effective change in the gate voltage. By considering the transconductance g_m of the transistor, the amplitude of the fraction of the action potential that is actually transduced, i.e. which is coupled to the EGFET gating, can be estimated as $\Delta V_{AP} = \frac{\Delta I_{DS}}{g_m}$. Such amplitude ranges between 1 and 3 mV, a considerable fraction of AP amplitude, and

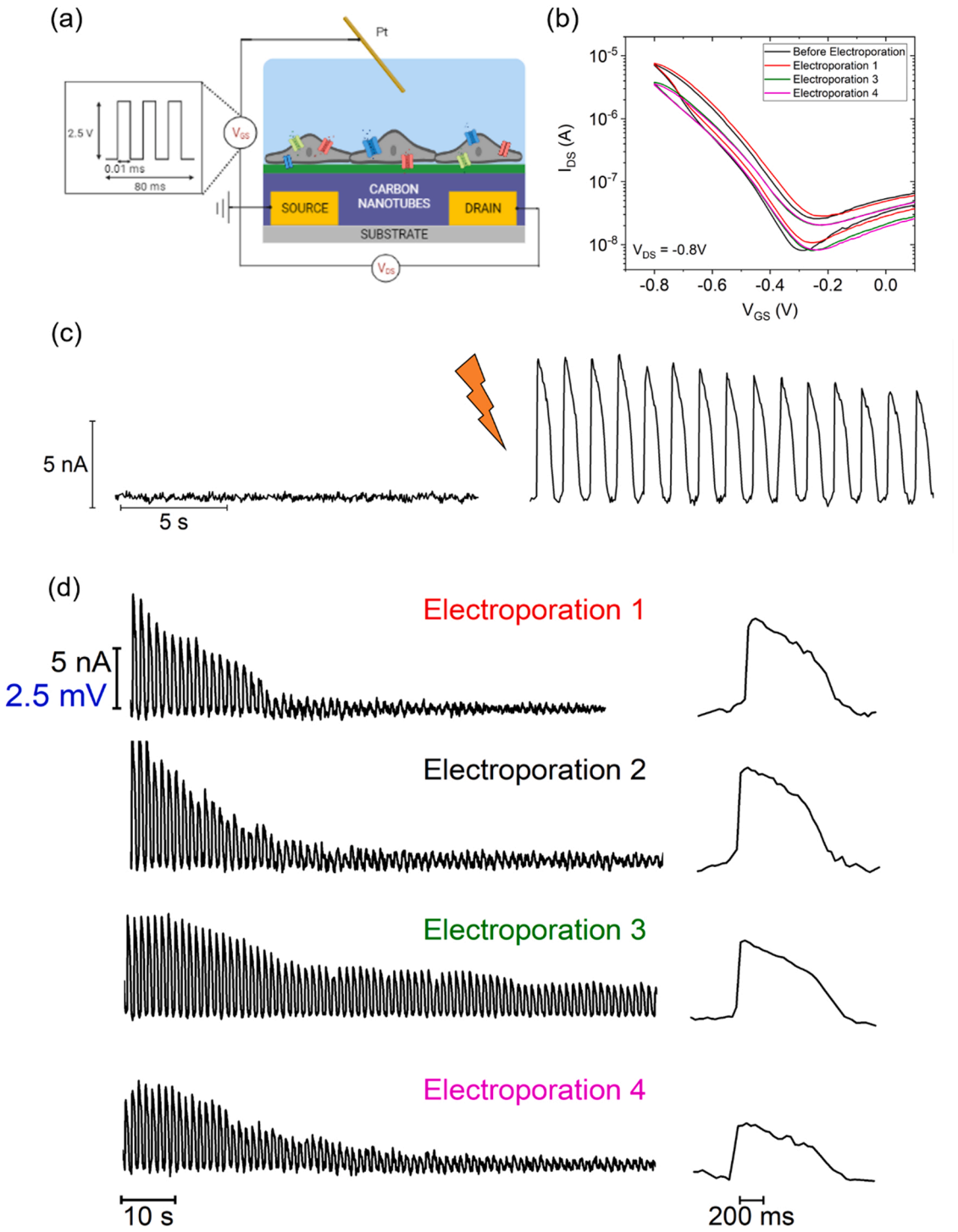

Fig. 4. Electroporation using planar EGFETs (a) Schematic of the EGFET depicting how electroporation was applied (b) Effect of electroporation on transistor performance (c) In the case of the transistors where spontaneous intracellular-like recording was not obtained, electroporation was introduced using planar EGFETs. (d) Multiple electroporation of the same cell using the same EGFET.

comparable to recently reported works that employ electro [31] or optoporation [35]. The signal to noise ratio SNR of the signals recorded in the I_{DS} (Fig. 3a) trace is 44 dB. Because of the change in the effective gate potential of the transistor caused by the cellular activity, spikes in the leakage gate current are also observed. A zoomed picture of an I_{DS} trace together with the corresponding gate leakage spikes is shown in Fig. 3(b). We can clearly observe that the acquired I_{DS} signal shows the characteristic shape and duration of an AP from human-derived cardiomyocytes [26]. The AP duration measured at 50% amplitude (APD50) is ~500 ms as expected for hiPSC-CMs [26]. In Fig. 3(c), one can distinguish the different phases of ion flow inward and outward the cell. The five phases represent, respectively, the opening of fast Na^+ channels (depolarization phase 0), the transient outwards K^+ channels (short repolarization phase 1), the slow inward Ca^{2+} channels (plateau phase 2) and the K^+ channels (depolarization phase 3 and resting potential phase 4). Instead, the gate current spike resembles a pure capacitive current due to an immediate change in potential. In particular, the first larger peak in I_{GS} occurs exactly at the cardiac upstroke

(depolarization), as observed in the overlapped I_{DS} trace, whereas the subsequent smaller peak occurs at the end of the repolarization phase. This demonstrates that we can spontaneously record both the extra and intracellular activity of the cell simultaneously in one single recording by monitoring I_{GS} and I_{DS}. Such spontaneous recording of intracellular-like APs is a remarkable observation, since previous reports have shown that without any external stimuli, EGFETs record mainly extracellular field potentials [18,19,36].

Supplementary material related to this article can be found online at doi:10.1016/j.snb.2023.134227.

Spontaneous recordings of intracellular-like APs were achieved on several transistors over 6 different samples and distributed in 3 independent cell preparations. Other examples of spontaneous AP recordings can be seen in Fig. 3(e, f). The amplitude and frequency of the signals varies among cell cultures according to the expected variability in cell adhesion and in beating frequency. Also, we did not observe noticeable differences in recordings obtained with transistors of different channel width (146 or 64 μm). The example in Fig. 3(e) shows APs every 1.7 s while that in Fig. 3f every 5 s, in agreement with the beating rates observed from optical monitoring of the cardiac cells. Variability of the beating frequency across different cell preparations was due to the fact that our custom-made acquisition system was not designed to precisely control cell temperature. We also note that the current modulation cannot be explained with the mechanical contraction of cells, since in this case every single EGFET should show the same signal given the full coverage of the culture. Fig. 3(f) depicts the two main mechanisms that we suggest as responsible for enabling recordings of AP from cardiac cells in our SWCNTs EGFETs. On the one hand, cells may wrap completely SWCNTs patches that protrude outside fibronectin, creating a full engulfment that has been shown to lead to intracellular-like recordings in previous literature [37,38]. On the other hand, the extremely small diameter of SWCNTs may lead to spontaneous internalization and to direct contact between SWCNTs and cytosol [39]. In a previous work, Zhao et al. already demonstrated that U shape Nanowire FETs are able to record an almost full amplitude AP thanks to the internalization of the nanowire by the cell [8]. Because the two mechanisms lead both to the internalization of SWCNTs by the cell, we do not expect performance differences in terms of signal amplitude and quality of intracellular-like AP recordings. This hypothesis will be tested with future extensive experiments aimed at clarifying the semiconductor/cells interface at nanoscale level.

3.4. Electroporation of cardiac cells using planar EGFET

In some cases, we did not detect any AP despite of the contraction of adherent cardiomyocytes on the planar EGFETs. This could be due to a non-optimal coupling of the cells with the active semiconducting phase related to the simplicity of the device fabrication and interface creation, an aspect that requires further investigations in the future. In such instances, we attempted to perform cell electroporation in order to induce a more intimate coupling. Electroporation has been widely used with 3D nanostructures to open nanopores in the cellular membrane and thus get a direct electrical contact between sensing element and cytosol. As a consequence of electroporation, sensing elements such as electrodes or FETs are able to record directly the cellular potential instead of the extracellular field potential. In the case of planar EGFETs, nanopores in the cellular membrane created by electroporation enables direct modulation of the EGFET current by the cellular membrane potential. To achieve high electric fields passing through the cell membrane for electroporation, a train of monophasic pulses, with an amplitude of 2.5 V and a period of 200 μs, was applied for a total duration of 80 ms between the gate and the source of the transistor. The schematic of the device illustrating the electroporation methodology is depicted in Fig. 4(a). In Fig. 4c, we report experimental data on the application of such electroporation protocol. The signal shown in Fig. 4(c, left) does not present any current modulation. On the same device, the electroporation-induced recorded signals depicted in Fig. 4(c, right) immediately show the clear shape, duration, and frequency of APs, similar to the traces in Fig. 3(a). It should be noted that unlike previous reports, where electroporation is generally applied to high aspect ratio 3D nanostructures, in our experiment the SWCNT film is planar at the microscale apart from its nanostructured morphology as shown in the AFM figure (Fig. 2(a)). To check the stability of the transistor, transfer curves taken before and after 4 successive electroporation protocols are shown in Fig. 4(b), where we compare the EGFET electrical performance as a consequence of the applied fast pulses. As seen from the graph, there is no significant change in the transistor performance, confirming that EGFETs could be reliably used for cell electroporation or possibly stimulation for cardiac pacing. The electroporation-induced intracellular coupling lasted for about 1–2 min after which the amplitude of the signal decreased as seen also in previous reports [15]. Future improvements such as the implementation of 3D nanostructures, like hollow nanotubes [40] or nanovolcanoes [13], may be implemented to prolong the temporal stability of the intracellular coupling. Alternatively, the possibility to repeat the electroporation protocol on the same cells can also lead to prolonged intracellular recordings [41]. In this regard, we were able to electroporate the same cell using the same EGFET for multiple times as shown in Fig. 4(d), confirming that the procedure does not significantly degrade the cell-transistor coupling. Multiple electroporations were performed consecutively in the same measurement session within few minutes. Here, we highlight that APs after each electroporation show the same shape and duration. In Figure SI2 of the supporting information, we plot the calculated APD50 values versus the multiple electroporation cycles, demonstrating that the APD50 remains fairly constant. To check the effects of electroporation on the cells, we performed fluorescence live/dead assays after electroporation and recording (Supporting Information SI3). The fluorescence images confirm that cells survive the electroporation procedure.

4. Conclusion

To conclude, we have successfully fabricated arrays of EGFETs based on solution processed semiconducting SWCNT networks and used them to record APs from hiPSC-CMs. Remarkably, spontaneous recording of intracellular-like signals can be reproducibly obtained, not previously reported for any planar transistor technology. The optimal coupling between the channel of the EGFET and the cells allows the recording of a good fraction of the APs of about 1–3 mV. The recorded APs showed high signal-to-noise ratio of 44 dB for the spontaneous recording and resembled closely the typical electrophysiological signals from human-derived cardiomyocytes. The capability to record APs as typically obtained with intracellular recordings is attributed to the tight coupling between cells and SWCNTs that leads to engulfment and possibly to spontaneous internalization of carbon nanowires into the cardiac cells. Given the randomly protruding topography of SWCNTs, we suggest that Fibronectin gel may not coat uniformly and completely the network. However, the precise mechanism will be the subject of extended future studies. In future works, the cell-EGFET coupling could be improved following two main strategies. On the one hand, different adhesion factors or functionalizations could be tested to improve the cellular adhesion on the semiconducting material or to obtain similar adhesion with a thinner functionalization layer. On the other hand, device morphology can be modified to enhance the coupling between the SWCNTs and the cells. For example, a different coating method of SWCNTs can result in a much rougher surface, with a larger number of SWCNT protruding from the functionalization, or by increasing the height of the protruding SWCNTs to increase the probability of cellular engulfment [39,42].

Moreover, we were also able to induce the cell-EGFET coupling on-demand by applying a cell electroporation protocol that enabled recordings of APs from cells that did not spontaneously produced sufficient coupling with carbon nanotubes. The electroporation process

could be repeated several times on the same cardiac cell, highlighting the low invasiveness of the procedure.

The EGFETs were produced with solution processed active materials and using cost-effective fabrication methods such as spin-coating. The exploitation of such materials and methods is very promising toward flexible large-area biosensors arrays for monitoring and mapping of electrogenic cell cultures activity, in-vivo biomedical applications or disposable devices for pharmacological screenings. Moreover, EGFETs have the potential to be employed as multifunctional sensors for detecting pH changes and biomarkers combined with electrophysiological recording.

CRediT authorship contribution statement

Mario Caironi and Francesco De Angelis designed the experiments. Alireza Molazemhosseini, Fabrizio Antonio Viola, Michele Dipalo and Francesco Modena fabricated the EGFETs. Giuseppina Iachetta cultured the cells and carried out the fluorescence imaging. Nicolas F. Zorn and Felix J. Berger from Jana Zaumseil's group prepared and provided the SWCNTs. Adrica Kyndiah, Fabrizio Antonio Viola and Michele Dipalo carried out the cell recording experiments. Adrica Kyndiah analysed the electrical recording data. The manuscript was written, reviewed and edited by Adrica Kyndiah, Michele Dipalo, Mario Caironi and Francesco De Angelis.

Declaration of Competing Interest

The authors declare that they have no known competing financial interests or personal relationships that could have appeared to influence the work reported in this paper.

Data availability

Data will be made available on request.

Acknowledgements

This work was partially supported by the European Union's Horizon 2020 Research and Innovation Programme "Electronic Smart Systems - SiMBiT: Single molecule bio-electronic smart system array for clinical testing", grant agreement number 824946, by the European Union's H2020-EU.4.b. - Twinning of research institutions "GREENELIT", grant agreement number 951747, and by the European Union's H2020 Research and Innovation Programme "TOX-Free", grant agreement number 964518. The fabrication of the devices was partially carried out at PoliFab, the micro- and nano-technology center of the Politecnico di Milano. We thank Prof. Tobias Cramer for sharing with us the software for the device characterisation and recording. This work was performed within the Sustainability Activity of Istituto Italiano di Tecnologia.

Appendix A. Supporting information

Supplementary data associated with this article can be found in the online version at doi:10.1016/j.snb.2023.134227.

References

[1] P. Orvos, Z. Kohajda, J. Szlovák, P. Gazdag, D.T. Tamás Árpádffy-Lovas, A. Geramipour, L. Tálosi, N. Jost, A. Varró, L. Virág, Evaluation of possible proarrhythmic potency: comparison of the effect of dofetilide, cisapride, sotalol, terfenadine, and verapamil on hERG and native IKR currents and on cardiac action potential, Toxicol. Sci. (2018), https://doi.org/10.1093/toxsci/kfy299.

[2] M. Taketani, M. Baudry, Advances in Network Electrophysiology, Springer,, US, 2006, https://doi.org/10.1007/b136263.

[3] P. Fromherz, A. Offenhausser, T. Vetrrer, A neuron-silicon junction: a retzius cell of the leech on an insulated-gate field-effect transistor, Sci. (80-.) 252 (1978).

[4] C. Sprössler, M. Denyer, S. Britland, W. Knoll, A. Offenhäusser, Electrical recordings from rat cardiac muscle cells using field-effect transistors, Phys. Rev. E - Stat. Phys., Plasmas, Fluids, Relat. Interdiscip. Top. 60 (1999) 2171–2176, https://doi.org/10.1103/PhysRevE.60.2171.

[5] D. Khodagholy, T. Doublet, P. Quilichini, M. Gurfinkel, P. Leleux, A. Ghestem, E. Ismailova, T. Hervé, S. Sanaur, C. Bernard, G.G. Malliaras, In vivo recordings of brain activity using organic transistors, Nat. Commun. 4 (2013), https://doi.org/10.1038/ncomms2573.

[6] A.H. Wu, Cardiotoxic drugs: Clinical monitoring and decision making, Heart 94 (2008) 1503–1509, https://doi.org/10.1136/hrt.2007.133876.

[7] X. Duan, R. Gao, P. Xie, T. Cohen-Karni, Q. Qing, H.S. Choe, B. Tian, X. Jiang, C. M. Lieber, Intracellular recordings of action potentials by an extracellular nanoscale field-effect transistor, Nat. Nanotechnol. 7 (2012) 174–179, https://doi.org/10.1038/nnano.2011.223.

[8] Y. Zhao, S.S. You, A. Zhang, J.H. Lee, J. Huang, C.M. Lieber, Scalable ultrasmall three-dimensional nanowire transistor probes for intracellular recording, Nat. Nanotechnol. 14 (2019) 783–790, https://doi.org/10.1038/s41565-019-0478-y.

[9] N. Hu, D. Xu, J. Fang, H. Li, J. Mo, M. Zhou, B. Li, H. jiuan Chen, T. Zhang, J. Feng, T. Hang, W. Xia, X. Chen, X. Liu, G. He, X. Xie, Intracellular recording of cardiomyocyte action potentials by nanobranched microelectrode array, Biosens. Bioelectron. 169 (2020), 112588, https://doi.org/10.1016/j.bios.2020.112588.

[10] P.B. Kruskal, Z. Jiang, T. Gao, C.M. Lieber, Beyond the patch clamp: Nanotechnologies for intracellular recording, Neuron 86 (2015) 21–24, https://doi.org/10.1016/j.neuron.2015.01.004.

[11] J. Fang, D. Xu, H. Wang, J. Wu, Y. Li, T. Yang, C. Liu, N. Hu, Scalable and Robust Hollow Nanopillar Electrode for Enhanced Intracellular Action Potential Recording, Nano Lett. 23 (2023) 243–251, https://doi.org/10.1021/acs.nanolett.2c04222.

[12] D. Braeken, D. Jans, R. Huys, A. Stassen, N. Collaert, L. Hoffman, W. Eberle, P. Peumans, G. Callewaert, Open-cell recording of action potentials using active electrode arrays, Lab Chip 12 (2012) 4397–4402, https://doi.org/10.1039/c2lc40656j.

[13] B.X.E. Desbiolles, E. De Coulon, A. Bertsch, S. Rohr, P. Renaud, Intracellular recording of cardiomyocyte action potentials with nanopatterned volcano-shaped microelectrode arrays, Nano Lett. 19 (2019) 6173–6181, https://doi.org/10.1021/acs.nanolett.9b02209.

[14] J. Abbott, T. Ye, L. Qin, M. Jorgolli, R.S. Gertner, D. Ham, H. Park, CMOS nanoelectrode array for all-electrical intracellular electrophysiological imaging, Nat. Nanotechnol. 12 (2017) 460–466, https://doi.org/10.1038/nnano.2017.3.

[15] C. Xie, Z. Lin, L. Hanson, Y. Cui, B. Cui, Intracellular recording of action potentials by nanopillar electroporation, Nat. Nanotechnol. 7 (2012) 185–190, https://doi.org/10.1038/nnano.2012.8.

[16] M. Dipalo, G. Melle, L. Lovato, A. Jacassi, F. Santoro, V. Caprettini, A. Schirato, A. Alabastri, D. Garoli, G. Bruno, F. Tantussi, F. De Angelis, A. Jacassi, M. Dipalo, A. Alabastri, D. Garoli, L. Lovato, A. Schirato, G. Melle, F. De Angelis, V. Caprettini, F. Santoro, Plasmonic meta-electrodes allow intracellular recordings at network level on high-density CMOS-multi-electrode arrays, Nat. Nanotechnol. 13 (2018) 965–971, https://doi.org/10.1038/s41565-018-0222-z.

[17] M. Dipalo, H. Amin, L. Lovato, F. Moia, V. Caprettini, G.C. Messina, F. Tantussi, L. Berdondini, F. De Angelis, Intracellular and extracellular recording of spontaneous action potentials in mammalian neurons and cardiac cells with 3D plasmonic nanoelectrodes, Nano Lett. 17 (2017) 3932–3939, https://doi.org/10.1021/acs.nanolett.7b01523.

[18] A. Spanu, A. Bonfiglio, Interfacing cells with organic transistors: a review of in vitro and in vivo applications, Lab Chip 21 (2021) 795–820, https://doi.org/10.1039/d0lc01007c.

[19] A. Kyndiah, F. Leonardi, C. Tarantino, T. Cramer, R. Millan-Solsona, E. Garreta, N. Montserrat, M. Mas-Torrent, G. Gomila, Bioelectronic Recordings of Cardiomyocytes with Accumulation Mode Electrolyte Gated Organic Field Effect Transistors, Biosens. Bioelectron. 150 (2020), 111844, https://doi.org/10.1016/j.bios.2019.111844.

[20] T. Cramer, B. Chelli, M. Murgia, M. Barbalinardo, E. Bystrenova, D.M. De Leeuw, F. Biscarini, Organic ultra-thin film transistors with a liquid gate for extracellular stimulation and recording of electric activity of stem cell-derived neuronal networks, Phys. Chem. Chem. Phys. 15 (2013) 3897–3905, https://doi.org/10.1039/c3cp44251a.

[21] F. Torricelli, D.Z. Adrahtas, Z. Bao, M. Berggren, F. Biscarini, A. Bonfiglio, C. A. Bortolotti, C.D. Frisbie, E. Macchia, G.G. Malliaras, I. McCulloch, M. Moser, T.-Q. Nguyen, R.M. Owens, A. Salleo, A. Spanu, L. Torsi, Electrolyte-gated transistors for enhanced performance bioelectronics, Nat. Rev. Methods Prim. 1 (2021), https://doi.org/10.1038/s43586-021-00065-8.

[22] E. Masvidal-Codina, X. Illa, M. Dasilva, A.B. Calia, T. Dragojević, E.E. Vidal-Rosas, E. Prats-Alfonso, J. Martínez-Aguilar, J.M. De la Cruz, R. Garcia-Cortadella, P. Godignon, G. Rius, A. Camassa, E. Del Corro, J. Bousquet, C. Hébert, T. Durduran, R. Villa, M.V. Sanchez-Vives, J.A. Garrido, A. Guimerà-Brunet, High-resolution mapping of infraslow cortical brain activity enabled by graphene microtransistors, Nat. Mater. 18 (2019) 280–288, https://doi.org/10.1038/s41563-018-0249-4.

[23] C. Pitsalidis, A.M. Pappa, A.J. Boys, Y. Fu, C.M. Moysidou, D. Van Niekerk, J. Saez, A. Savva, D. Iandolo, R.M. Owens, Organic Bioelectronics for in Vitro Systems, Chem. Rev. 122 (2021) 4700–4790, https://doi.org/10.1021/acs.chemrev.1c00539.

[24] F.A. Viola, J. Barsotti, F. Melloni, G. Lanzani, Y.H. Kim, V. Mattoli, M. Caironi, A sub-150-nanometre-thick and ultraconformable solution-processed all-organic transistor, Nat. Commun. 12 (2021), https://doi.org/10.1038/s41467-021-26120-2.

[25] R.R. Søndergaard, M. Hösel, F.C. Krebs, Roll-to-Roll fabrication of large area functional organic materials, J. Polym. Sci. Part B Polym. Phys. 51 (2013) 16–34, https://doi.org/10.1002/polb.23192.
[26] G. Iachetta, N. Colistra, G. Melle, L. Deleye, F. Tantussi, F. De Angelis, M. Dipalo, Improving reliability and reducing costs of cardiotoxicity assessments using laser-induced cell poration on microelectrode arrays, Toxicol. Appl. Pharmacol. 418 (2021), https://doi.org/10.1016/j.taap.2021.115480.
[27] A. Barbaglia, M. Dipalo, G. Melle, G. Iachetta, L. Deleye, A. Hubarevich, A. Toma, F. Tantussi, F. De Angelis, Mirroring action potentials: label-free, accurate, and noninvasive electrophysiological recordings of human-derived cardiomyocytes, Adv. Mater. 33 (2021), https://doi.org/10.1002/adma.202004234.
[28] T. Cramer, A. Kyndiah, M. Murgia, F. Leonardi, S. Casalini, F. Biscarini, Double layer capacitance measured by organic field effect transistor operated in water, Appl. Phys. Lett. 100 (2012), 143302, https://doi.org/10.1063/1.3699218.
[29] A. Kyndiah, M. Checa, F. Leonardi, R. Millan-solsona, M. Di Muzio, S. Tanwar, L. Fumagalli, M. Mas-torrent, G. Gomila, Nanoscale mapping of the conductivity and interfacial capacitance of an electrolyte-gated organic field-effect transistor under operation, Adv. Funct. Mater. 2008032 (2020) 1–8, https://doi.org/10.1002/adfm.202008032.
[30] F.A. Viola, F. Melloni, A. Molazemhosseini, F. Modena, M. Sassi, L. Beverina, M. Caironi, A n-type, stable electrolyte gated organic transistor based on a printed polymer, Adv. Electron. Mater. 2200573 (2022), https://doi.org/10.1002/aelm.202200573.
[31] Y. Jimbo, D. Sasaki, T. Ohya, S. Lee, W. Lee, F. Arab Hassani, T. Yokota, K. Matsuura, S. Umezu, T. Shimizu, T. Someya, An organic transistor matrix for multipoint intracellular action potential recording, Proc. Natl. Acad. Sci. U. S. A. 118 (2021) 1–8, https://doi.org/10.1073/pnas.2022300118.
[32] A. Molazemhosseini, F.A. Viola, F.J. Berger, N.F. Zorn, J. Zaumseil, M. Caironi, A Rapidly Stabilizing Water-Gated Field-Effect Transistor Based on Printed Single-Walled Carbon Nanotubes for Biosensing Applications, ACS Appl. Electron. Mater. 3 (2021) 3106–3113, https://doi.org/10.1021/acsaelm.1c00332.
[33] F. Scuratti, G.E. Bonacchini, C. Bossio, J.M. Salazar-Rios, W. Talsma, M.A. Loi, M. R. Antognazza, M. Caironi, Real-time monitoring of cellular cultures with electrolyte-gated carbon nanotube transistors, ACS Appl. Mater. Interfaces 11 (2019) 37966–37972, https://doi.org/10.1021/acsami.9b11383.
[34] A. Graf, Y. Zakharko, S.P. Schießl, C. Backes, M. Pfohl, B.S. Flavel, J. Zaumseil, Large scale, selective dispersion of long single-walled carbon nanotubes with high photoluminescence quantum yield by shear force mixing, Carbon N. Y 105 (2016) 593–599, https://doi.org/10.1016/j.carbon.2016.05.002.
[35] M. Dipalo, S.K. Rastogi, L. Matino, R. Garg, J. Bliley, G. Iachetta, G. Melle, R. Shrestha, S. Shen, F. Santoro, A.W. Feinberg, A. Barbaglia, T. Cohen-Karni, F. de Angelis, Intracellular action potential recordings from cardiomyocytes by ultrafast pulsed laser irradiation of fuzzy graphene microelectrodes, Sci. Adv. 7 (2021) 1–10, https://doi.org/10.1126/SCIADV.ABD5175.
[36] F. Hempel, J.K.Y. Law, T.C. Nguyen, W. Munief, X. Lu, V. Pachauri, A. Susloparova, X.T. Vu, S. Ingebrandt, PEDOT:PSS organic electrochemical transistor arrays for extracellular electrophysiological sensing of cardiac cells, Biosens. Bioelectron. 93 (2017) 132–138, https://doi.org/10.1016/j.bios.2016.09.047.
[37] N. Shmoel, N. Rabieh, S.M. Ojovan, H. Erez, E. Maydan, M.E. Spira, Multisite electrophysiological recordings by self-assembled loose-patch-like junctions between cultured hippocampal neurons and mushroom-shaped microelectrodes, Sci. Rep. 6 (2016) 1–11, https://doi.org/10.1038/srep27110.
[38] A. Hai, J. Shappir, M.E. Spira, In-cell recordings by extracellular microelectrodes, Nat. Methods 7 (2010) 200–202, https://doi.org/10.1038/nmeth.1420.
[39] R. Capozza, V. Caprettini, C.A. Gonano, A. Bosca, F. Moia, F. Santoro, F. De Angelis, Cell membrane disruption by vertical micro-/nanopillars: role of membrane bending and traction forces, ACS Appl. Mater. Interfaces 10 (2018) 29107–29114, https://doi.org/10.1021/acsami.8b08218.
[40] Z.C. Lin, C. Xie, Y. Osakada, Y. Cui, B. Cui, Iridium oxide nanotube electrodes for sensitive and prolonged intracellular measurement of action potentials, Nat. Commun. 5 (2014) 1–10, https://doi.org/10.1038/ncomms4206.
[41] J. Lee, T. Gänswein, H. Ulusan, V. Emmenegger, A.M. Saguner, F. Duru, A. Hierlemann, Repeated and on-demand intracellular recordings of cardiomyocytes derived from human-induced pluripotent stem cells, ACS Sens. 7 (2022) 3181–3191, https://doi.org/10.1021/acssensors.2c01678.
[42] R. Capozza, L. Giomi, C.A. Gonano, F. De Angelis, How to puncture a biomembrane: elastic versus entropic rupture, 2019: 3–7.

Adrica Kyndiah obtained her PhD degree from the Alma Mater Studorium Università di Bologna in April 2015. Her thesis was focused on the study of charge transport at the various interfaces of an Organic Field Effect Transistor. She worked as a postdoctoral researcher at several international labs including the French Alternative Energies and Atomic Energy Commission (CEA) in Grenoble and the IMS lab at the Centre Nationnal de la Recherche Scientifique (CNRS) in Bordeaux, France. In 2017 she won the Marie Curie postdoctoral fellowship and joined the Nanoscale Bioelectrical Characterization group of at the Institute of Bioengineering of Catalonia IBEC in Barcelona Spain. She joined the Istituto Italiano di Tecnologia as a researcher in July 2020 where she is focusing her research activity on the development of carbon–based electrolyte gated transistors for biosensors and bioelectronics.

Michele Dipalo received his Ph.D. Degree in Electrical engineering from the Electron Devices and Circuits Department at the University of Ulm in Germany. From 2013, he works at the Italian Institute of Technology in Genova (Italy), where he develops novel electrophysiological techniques based on 3D nanostructures and applies nano-optics and plasmonics to in vitro extracellular and intracellular network recordings.

Alireza Molazemhosseini received his PhD in Materials Engineering from Politecnico di Milano (Milan, Italy) in 2017. His thesis was focused on development of electrochemical biosensors for point-of-care applications. In 2018, he joined the Center for Nano Science and Technology (CNST) of the Italian Institute of Technology (IIT, Milan, Italy) as a post-doc fellow where he developed carbon-based electrolyte gated field effect transistors for biosensing applications. His research interests focus on electrical and electrochemical sensing platforms for biomedical applications.

Fabrizio Antonio Viola received his MS degree in electronic engineering in 2014 and obtained his Ph.D. in Bioengineering and Robotics at the University of Genova, working on multimodal tactile sensors based on organic field-effect transistors. In 2018 he joined the group of Dr. Mario Caironi (Printed and Molecular Electronics) as Postdoc Researcher at Center for Nano Science and Technology @Politecnico di Milano of the Istituto Italiano di Tecnologia, working for 4 years on printed electronics, bioelectronics and epidermal electronics. He is currently Research Associate at University of Cagliari, and a 2022 MUR Young Researchers – SoE grantee. His main interests are printed electronics, bioelectronics and ultra-thin/epidermal electronics and for the health care.

Francesco Modena received his MS degree in materials engineering and nanotechnology in 2016, and his PhD in electronics at the department of electronics, information and biotechnologies (DEIB) of Politecnico di Milano in 2022. He is currently working as a Post-Doc in the Printed and Molecular Electronics group of Dr. Mario Caironi at the Center for Nano Science and Technology@PoliMi (CNST) of the Istituto Italiano di Tecnologia (IIT, Milan, Italy). His main interests are printed electronics, microfabrication and integration of biomedical sensors for diagnosis and health care applications.

Giuseppina Iachetta received her Ph.D. Degree in Advanced Biology from the University of Naples Federico II. Presently, she works as post-doc in the Plasmon Nanotechnologies group at the Italian Institute of Technology (Genova, Italy). Her research interests focus on new technologies for pre-clinical cardiotoxicity and neurotoxicity screenings in vitro.

Nicolas F. Zorn is a doctoral student in the group of Jana Zaumseil at Heidelberg University. His research focusses on light emission and charge transport in optoelectronic devices with covalently functionalized carbon nanotubes.

Felix J. Berger received his PhD from the University of Heidelberg in 2021 with a work on luminescent defects in single-walled carbon nanotubes. His research interests include light-emitting and light-harvesting devices based on novel materials.

Jana Zaumseil received her Ph.D. in physics in 2007 from the University of Cambridge (UK). Since 2014 she is a full professor for Applied Physical Chemistry at Heidelberg University (Germany). Her research interests include functionalization and processing of semiconducting carbon nanotubes for charge transport and light-matter interactions.

Mario Caironi obtained his Ph.D. in Information Technology with honours at Politecnico di Milano (Milan, Italy). In 2007 he joined the group of Prof. Sirringhaus at the Cavendish Lab. (Cambridge, UK) as a post-doc, working for 3 years on high resolution printing of downscaled organic transistors and circuits, and on charge transport in high mobility polymers. In 2010 he was appointed as Team Leader at the Center for Nano Science and Technology@PoliMi (CNST) of the Istituto Italiano di Tecnologia (IIT, Milan, Italy), obtaining tenure in 2019. He is currently interested in printed organic and hybrid micro- and opto-electronics, thermoelectrics, bioelectronics, and sustainable and edible electronics. He is a 2014 ERC Starting grantee and a 2019 ERC Consolidator grantee.

Francesco De Angelis received his Ph.D. Degree in Physics from the University "Roma Tre" of Rome in Italy. He is currently Principal Investigator at the Italian Institute of Technology (Genova, Italy), where he leads the Plasmon Nanotechnologies group. His research interests focus on nanotechnologies and nano-optics applied to bio-applications, from sequencing of DNA and proteins to biosensing and electrophysiological recordings of neurons and cardiomyocytes.